EXTRACAPSULAR EXTENSION RISK ASSESSMENT USING AN ARTIFICIAL INTELLIGENCE PROSTATE CANCER MAPPING ALGORITHM

Alan Priester[1,2,*], Sakina M. Mota[2], Joshua Shubert[2], Shyam Natarajan[1,2], Wayne G. Brisbane[1]
[1] *University of California, Los Angeles;* [2] *Avenda Health, Inc;* [*] *alan@avendahealth.com*

Introduction and Background: The presence of extraprostatic extension (ECE) is critical to risk stratification and management of prostate cancer (PCa), including determination of treatment eligibility and surgical margins. Current techniques for prediction of ECE, which rely upon interpretation of magnetic resonance imaging (MRI) and clinical data such as Gleason Grade group (GG) and prostate specific antigen (PSA), are imperfect. Herein we evaluate the use of an artificial intelligence (AI) cancer mapping algorithm to improve ECE risk assessment.

Specific Aims: Compare the ECE predictive accuracy of AI versus conventional techniques.

Methods and Materials: Consecutively accrued patients who received preoperative multiparametric MRI, confirmatory biopsy, and subsequent prostatectomy were evaluated (N = 121). A radiologist prospectively interpreted the MRI, defining regions of interest (ROIs) suspicious for PCa and ECE risk via a Likert scale. Following prostatectomy, a pathologist determined if and where ECE occurred using whole-mount slides (Fig B). An FDA-cleared AI cancer mapping algorithm (Unfold AI, K221624) was then investigated for ECE prediction. The algorithm incorporated T2-weighted MRI, serum PSA, and biopsy histopathology to generate 3D cancer estimation maps for each case. ECE risk was estimated as the total cancer probability of voxels intersecting and up to 2 mm beyond the prostate capsule (Fig A). For comparison, conventional metrics were also assessed: GG, serum PSA, MRI Likert score, Partin table value, and ROI capsular contact length. A receiver operator characteristic was generated for each metric, and areas under the curve (AUCs) were compared using DeLong's test at $\alpha = 0.05$.

Results: The distribution of GG on final diagnosis was 13% GG1, 56% GG2, 16% GG3, 9% GG4, and 6% GG5. ECE was present in 46/121 cases; of these, 76% had posterior ECE only, 15% had anterior ECE only, and 9% had both. The receiver operator characteristic for patient-level ECE prediction is shown in Fig C. The AUC of AI (0.88) was significantly higher ($p < 0.001$) than PSA (0.60), GG (0.68), MRI Likert score (0.71), and Partin tables (0.65). The AUC of AI was likewise higher than ROI contact length (0.83), an improvement that was suggestive but insufficient for statistical significance ($p = 0.10$).

Discussion and Conclusion: Unlike conventional ECE predictors, AI can combine multi-modal data to map cancer risk in 3D. This approach shows promise as a means of ECE prediction, surpassing conventional methodology such as Partin tables and subjective MRI interpretation. Clinicians furnished with AI could potentially improve prostate cancer management, patient outcomes, and quality of life. This approach shows considerable promise and warrants further study in broader populations.

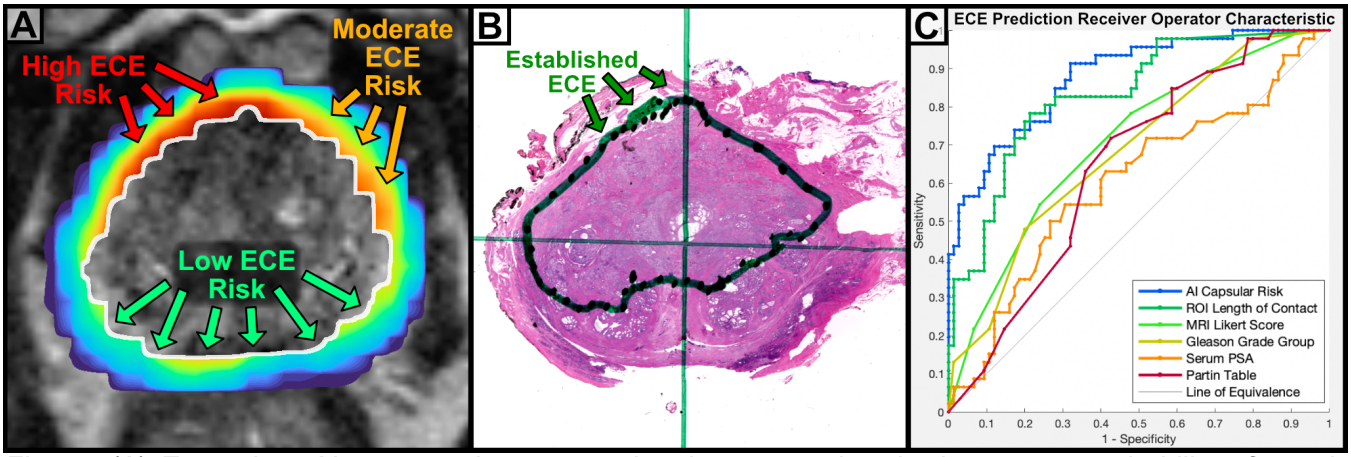

Figure: (A) Exemplary AI-generated cancer estimation map, wherein the cancer probability of voxels intersecting and beyond the capsule was used to make an objective assessment of ECE risk. (B) Exemplary ground truth histopathology slide wherein ECE was observed in the prostate anterior, the highest-risk region identified by the AI algorithm. (C) Receiver operator characteristic for patient-level prediction of ECE using AI and conventional metrics.